

Pressure effect on the electronic structure of $\text{La}_{5/3}\text{Sr}_{1/3}\text{NiO}_4$ by XES and RIXSL. Simonelli,^{1,*} V. M. Giordano,² N. L. Saini,³ and G. Monaco¹¹*European Synchrotron Radiation Facility, BP220, FR-38043 Grenoble Cedex, France*²*Laboratoire de Physique de la Matière Condensée et Nanostructures (LPMCN)—UMR 5586—Université Lyon I, FR-69622 Villeurbanne Cedex, France*³*Dipartimento di Fisica, Università di Roma La Sapienza, P. le Aldo Moro 2, IT-00185 Roma, Italy*

(Received 1 August 2011; revised manuscript received 30 September 2011; published 28 November 2011)

We report a study of the pressure effect on the electronic properties of the $\text{La}_{5/3}\text{Sr}_{1/3}\text{NiO}_4$ system by x-ray emission spectroscopy and resonant inelastic x-ray scattering. We find that (i) the applied pressure induces a high-spin to low-spin transition and (ii) the hopping between the neighboring Ni sites with different oxidation states is strongly suppressed. Pressure effects on the occupied and unoccupied electronic states and on the corresponding electronic excitations are discussed.

DOI: [10.1103/PhysRevB.84.195140](https://doi.org/10.1103/PhysRevB.84.195140)

PACS number(s): 74.25.Jb, 75.25.Dk, 78.70.Ck, 71.27.+a

I. INTRODUCTION

The complex interplay between the spin-charge lattice of $\text{La}_{2-x}\text{Sr}_x\text{NiO}_4$ makes it a model system to study the role of these electronic degrees of freedom in various phenomena as stripe correlations and metal-insulator transitions.^{1–7} Resonant inelastic x-ray scattering (RIXS) is one of the powerful probes that can measure the charge and spin correlation functions multiplied by a resonant enhancement factor.^{8,9} RIXS in the hard- and soft-x-ray regimes is currently utilized to study various types of excitations in strongly correlated electron systems.^{10–21} Beyond the different range of momentum transfer, RIXS in the soft- and the hard-x-ray regimes shows differences in terms of relative intensity of the inelastic features. In particular, RIXS at the L edge of a transition-metal oxide (TMO) in the soft-x-ray regime shows stronger signal from the d - d excitations in comparison to the charge-transfer excitations and allows the study of magnon and bimagnon excitations at the same time. Instead, RIXS at the K edge of a TMO in the hard-x-ray regime shows weaker signal for the d - d excitations and stronger charge-transfer features, and it is sensitive only to bimagnon excitations.

Unlike soft x-rays, hard x-rays not only allow measurements in low-vacuum conditions with higher penetration depths but permit measurements in high-pressure conditions. Technically, RIXS at high pressure is still challenging, and to the best of our knowledge, only one pioneering work²² has been published so far. Otherwise, it is well known that pressure is one of the fundamental thermodynamic parameters controlling the fascinating physical properties of TMOs. In the particular case of $\text{La}_{5/3}\text{Sr}_{1/3}\text{NiO}_4$, it has been demonstrated that the stripe correlations are strongly affected by pressure²³ as in the case of isostructural cuprates²⁴ for which the correlation between stripe ordering and high- T_c superconductivity requires the understanding of charge-stripe dynamics. Incidentally, due to the difficulties of a high-pressure study, not many experiments have been performed on striped compounds. Nevertheless, high-pressure experiments open up possibilities to investigate new, theoretically predicted spin states²⁵ and to understand the stripe states in TMOs at low temperatures.^{1–6,20,21}

Recently, we reported a RIXS study in the hard-x-ray regime on the $\text{La}_{5/3}\text{Sr}_{1/3}\text{NiO}_4$ system, revealing a correlation

between the energetics of the d levels and the charge-stripe ordering.²¹ Here, we combine inelastic x-ray scattering, x-ray absorption, and x-ray emission spectroscopy (XES) to investigate the pressure effect on the different electronic excitations^{20,21,26} that resonate around the Ni K edge. We find that the hopping between neighboring Ni sites with different oxidation states in the system is suppressed and that a new spin state appears under high pressure. Additionally, we report significant pressure-induced changes in the charge-transfer resonating features detectable by RIXS.

II. EXPERIMENTAL DETAILS

A panoramic diamond-anvil cell was used with a $\text{La}_{5/3}\text{Sr}_{1/3}\text{NiO}_4$ -powder sample contained in a Be gasket together with neon as a pressure-transmitting medium to provide hydrostatic conditions. Additionally, a ruby was inserted in the cell for the pressure measurements. The RIXS experiments were performed at the Ni K edge at the ID16 beamline of the European Synchrotron Radiation Facility.²⁷ The scattering plane was horizontal, parallel to the linear polarization vector of the incoming x-ray beam. The spectrometer was based on a bent Si(551) analyzer crystal (bending radius $R = 1$ m) and a pixelated position-sensitive Medipix2 detector. The total energy resolution was 880 meV full width at half maximum. The XES data were acquired with the same spectrometer exciting the sample well above the Ni K edge and detecting the emitted fluorescence lines. The scattering angle 2θ was $\approx 90^\circ$ in order to minimize the nonresonant quasielastic peak. Measurements were made at several pressures in the range of 8–57 GPa, and a clear change in the spectra was observed between the ambient pressure and 8 GPa. A further increase in pressure hardly revealed any notable change, and hence, we report the highest-pressure data in comparison with the ambient-pressure data collected on the single crystal²¹ from which the powder was prepared. Comparing single-crystal and powder data is allowed due to the fact that the corresponding spectra are very similar when the single crystal is measured using an angle of 37° between the incoming beam and the c direction of the crystal as done in Ref. 21. This has been experimentally checked at ambient-pressure conditions.

III. RESULTS AND DISCUSSIONS

We start by presenting results of different electronic excitations influenced by pressure and resonating in the energy range around the Ni K edge. Figure 1 shows a two-dimensional RIXS map of intensity versus incident energy (E_1) and energy transfer, collected at ambient (AP) [Fig. 1(a)]²¹ and high pressures (HP) [Fig. 1(b)]. The different electronic excitations resonating at different E_1 are highlighted by boxes. For E_1 at the prepeak energy ($E_1 \approx 8.33$ keV), distinct resonances around 7 eV and 5 eV are found at AP [Fig. 1(a)] and HP [Fig. 1(b)]. At higher E_1 , fluorescence starts to dominate the spectra for energy-transfer values higher than 8 eV. Two inelastic peaks resonate at the main absorption edge ($E_1 \approx 8.345$ keV) with energy-transfer values of about 6 and 9 eV [Fig. 1(a)].

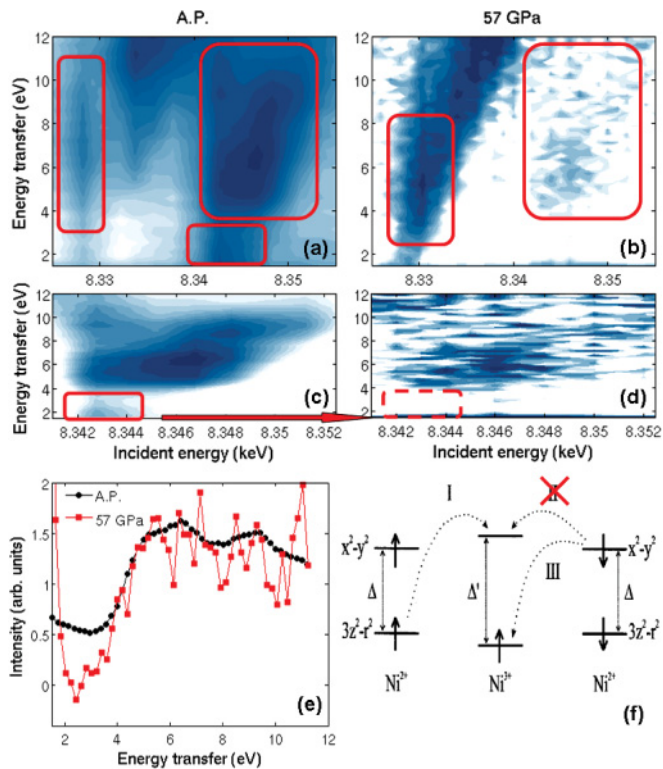


FIG. 1. (Color online) Contour plots of the RIXS intensity (logarithmic scale) as a function of incident energy around the Ni K edge and energy transfer at (a) ambient pressure and (b) 57 GPa. In the high-pressure data, the background coming from the high-pressure cell has been subtracted, using off-resonance spectra to estimate it. Different methods of background subtraction give the same results. The boxes mark the electronic excitations resonating with the incoming-photon energy at the absorption prepeak (≈ 8.33 keV) and main peak (≈ 8.345 keV). A rescaled zoom of the two-dimensional RIXS maps with the incoming-photon energy around the absorption main peak is reported at (c) ambient and (d) high pressures. (e) Inelastic intensity versus energy transfer for ambient pressure (dots) and high pressure (squares), obtained summing the maps in (c) and (d) over the incoming-photon-energy direction. The spectral weight at ≈ 2 eV is strongly suppressed under pressure. (f) Sketch of the simplified model representing the e_g orbitals at ambient pressure. The hopping between neighboring Ni sites with different oxidation states (II), which we have associated to the ≈ 2 eV excitation,²¹ is suppressed on applying pressure.

Applying pressure, the intensity of these two resonating features strongly decreases [Fig. 1(b)]. Finally, at AP a weak inelastic feature around 2 eV, which has been assigned to crystal-field ($d-d$) excitations,^{10,20,21} resonates mainly at the main-peak energy [Fig. 1(a)]. Applying pressure, this low-energy feature seems to disappear [Fig. 1(b)]. This can be better visualized in Figs. 1(c) and 1(d) in which we depict the RIXS maps at AP and HP respectively, rescaled in order to have comparable intensities for the inelastic features resonating around the main-peak energy; at HP in fact the signal is strongly suppressed. Integrating the RIXS maps reported in Figs. 1(c) and 1(d) over E_1 , we obtain the RIXS spectra in the traditional representation, i.e., intensity versus energy transfer [Fig. 1(e)]. The spectra collected at AP (dots) and HP (squares) overlap quite well except in the low-energy region, confirming the strong suppression of the $d-d$ excitations on applying pressure. Figure 1(f) shows the sketch of a simplified model representing the e_g orbitals at ambient pressure.^{5,21} In this model we distinguish between sites with (Ni^{3+}) and without (Ni^{2+}) dopant holes. Indeed, the site Ni^{3+} can be more correctly called $\text{Ni } 3d^8 \underline{L}$. Both representations have been used up to now since the $\text{Ni } 3d_{x^2-y^2}$ orbitals are hybridized with the O $2p_{xy}$ ones that host the hole site. The hopping between neighboring Ni sites with different oxidation states (II), which we have previously associated to the ≈ 2 eV excitation,²¹ is suppressed by applying pressure. This is in agreement with the following results.

Figure 2 shows the $K\beta$ x-ray emission spectra collected for $\text{La}_{5/3}\text{Sr}_{1/3}\text{NiO}_4$ at ambient (dots) and high pressures (squares).

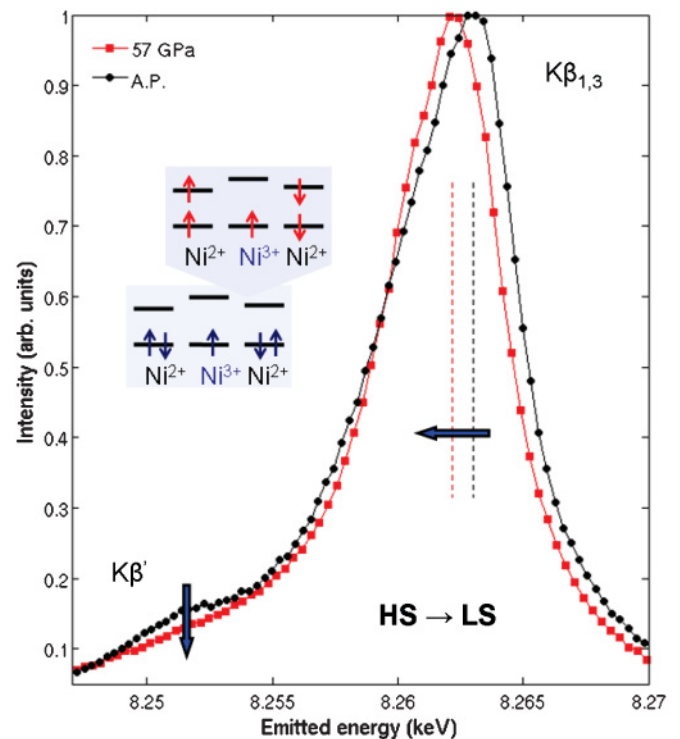


FIG. 2. (Color online) $K\beta$ x-ray emission lines measured for $\text{La}_{5/3}\text{Sr}_{1/3}\text{NiO}_4$ at ambient (dots) and high pressures (squares). While a clear shift of the $K\beta_{1,3}$ main line is observable, the intensity of the $K\beta'$ line decreases by applying pressure, consistent with a high-spin to low-spin transition.

The overall spectral shape of the $K\beta$ emission line is dominated by the $(3p,3d)$ exchange interaction. While a clear shift of the $K\beta_{1,3}$ main line is detectable, the intensity of the $K\beta'$ satellite decreases under pressure in agreement with a transition toward lower spin.²⁸ This has also been predicted theoretically by self-consistent Hartree-Fock calculations.²⁵ In the low-spin configuration, the hopping between the neighboring Ni sites with different oxidation states (II) is obviously suppressed.

In order to characterize the effect of the applied pressure on the occupied and unoccupied electronic states, we have exploited x-ray emission spectroscopy at the $K\beta$ satellite emission lines and partial fluorescence yield (PFY) absorption spectra, which is a high-resolution absorption spectra obtained by selecting the Ni $K\beta$ emission line and scanning E_1 across the Ni K edge. Figures 3(a) and 3(d) show the $K\beta$ satellite lines after the background subtraction at AP and HP, respectively. They correspond to the occupied states related to transitions to the $1s$ shell from the valence orbitals (mainly the Ni $3d$ hybridized with O $2p$ states). The Fermi energy (E_F) is indicated by a dashed line. Applying pressure, the density of states around the E_F increases, indicating a clear electronic delocalization. A comparison of the XES spectrum with the valence-band spectrum measured by photoemission and combined with the cluster calculations²⁹ allows us to identify different transition features.²⁶ The vertical lines indicate the position of different contributing electronic states. We can distinguish occupied Ni $3d$ states at ≈ 1.5 eV, O $2p$ nonbonding

and bonding states at ≈ 3 and 4 eV, and Ni $3d$ multiplet states at ≈ 6 eV from E_F .²⁶

Figures 3(b) and 3(e) show the Ni K -edge PFY absorption spectra measured at AP and HP, respectively, providing information on the unoccupied states. Different features in the absorption spectra can be identified as: (i) the pre-edge feature around 8.328 keV at AP and around 8.331 keV at HP, mainly due to Ni $1s$ to Ni $3d$ quadrupole transitions admixed with dipole contributions; (ii) the shoulder structure around 8.335 keV likely due to transitions from Ni $1s$ to the unoccupied states of p symmetry admixed with the electronic states derived from La $5d$ and Sr $4d$ in the continuum; and (iii) the main peak due to the Ni $1s$ to Ni $4p$ (admixed with O p orbitals) dipole transitions, appearing as a doublet structure with polarization sensitivity corresponding to different Ni-O distances.³⁰ Under pressure, the dipolar main peak is shifted to higher energy due to the volume contraction. At the same time, the prepeak rises toward higher energy. This can be due to the high-spin to low-spin transition; an increase of the e_g level splitting; or hybridization with the La $5d$ -Sr $4d$ levels, which could split under pressure due to the different ionic radii.

In between the Figs. 3(a) and 3(b), the horizontal lines represent the three charge-transfer (CT) excitations that we have identified by RIXS at AP [Fig. 3(c)]. Similarly, in between Figs. 3(d) and 3(e), the horizontal lines represent the CT transitions measured by RIXS at HP [Fig. 3(f)]. Applying

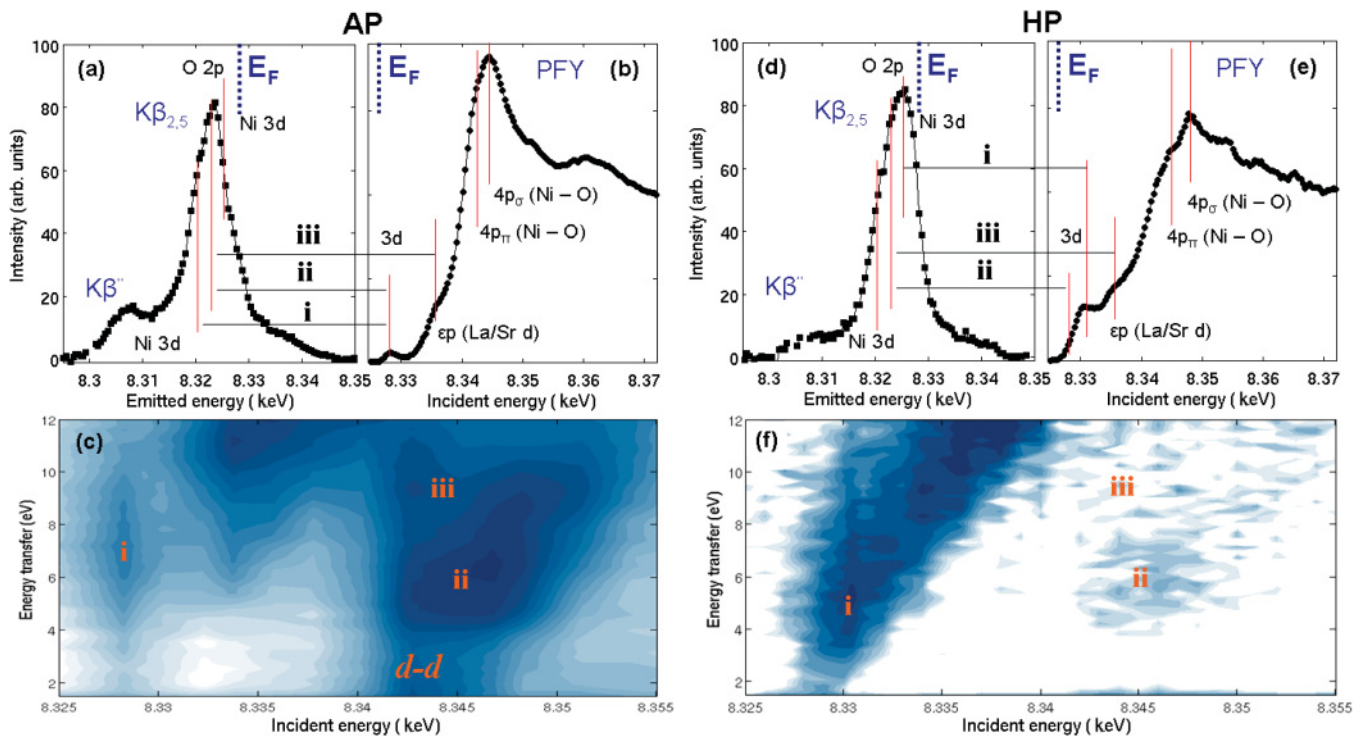


FIG. 3. (Color online) (a) and (d) $K\beta$ x-ray-emission satellite lines ($K\beta_{2,5}$) due to the transitions to the $1s$ shell from valence orbitals (Ni $3d$ hybridized with O $2p$), measured for $\text{La}_{5/3}\text{Sr}_{1/3}\text{NiO}_4$ at AP and HP, respectively. (b) and (e) display the Ni K -edge partial-fluorescence-yield absorption spectra at AP and HP, respectively, obtained by collecting the Fe $K\beta$ -emission yield as a function of the incident energy. The vertical lines indicate the approximate energy positions of the contributing electronic states. The Fermi energy (E_F) is indicated by a dashed line. The horizontal lines represent the three charge-transfer excitations that have been detected by RIXS, denoted by i , ii , and iii . Two-dimensional RIXS plots showing inelastic intensity versus incident energy and energy transfer at (c) ambient and (f) high pressures. Different CT transitions (i , ii , and iii) are indicated on top of the resonating excitations in the RIXS plots.

pressure, the inelastic feature resonating at the prepeak (*i*) changes in terms of resonating energy and energy transfer. The CT transition *i*, around 7 eV of energy transfer at AP, is likely due to the transition between the Ni $3d$ multiplet states and e_g levels. At HP, *i* is around 5 eV of energy transfer. This probably corresponds to the transition from t_{2g} to a new d state composed of e_g hybridized with the La $5d$ -Sr $4d$ levels. The change of the resonating energy when applying pressure is likely due to the growing of this new d state since the high- to low-spin transition suppresses the transition to the lower e_g level that is fully filled at HP. The transitions *ii* and *iii* resonating at the main-peak energy at about 6 and 9 eV of energy transfer, respectively, are present in both AP and HP measurements. Both transitions *ii* and *iii* result in doubling [Fig. 1(e)] by the double O $2p$ nonbonding and bonding occupied states at 3 and 4 eV from the E_F and by the splitting of the e_g unoccupied states. Transition *ii* is between the Ni $3d^9 \underline{L}$ (O $2p$) and e_g levels. Transition *iii* is between Ni $3d^9 \underline{L}$ (O $2p$) and La $5d$ and Sr $4d$ in the continuum. Both transitions *ii* and *iii* are weaker at higher pressure because of the high-spin to low-spin transition and likely correspond at HP only to the Ni^{3+} sites.

IV. SUMMARY AND CONCLUSIONS

In conclusion, we have investigated the electronic structure of $\text{La}_{5/3}\text{Sr}_{1/3}\text{NiO}_4$ by RIXS and XES under pressure. The applied pressure is found to induce a high-spin to low-spin transition. At the same time, hopping between neighboring Ni sites with different oxidation states shows a strong suppression under high pressure. Combining x-ray absorption and x-ray emission spectroscopy, we have provided a picture of the occupied and unoccupied states at ambient and high pressures. The inelastic features, which resonate in the RIXS spectra at different incoming-photon energies, have been assigned to different electronic transitions, and the pressure effect has been discussed. The results reported here clearly call for theoretical calculations to gain a more quantitative understanding of the present experimental results.

ACKNOWLEDGMENTS

The authors thank Simo Huotari and Takashi Mizokawa for the very fruitful discussions and S. W. Cheong for providing the high-quality sample for the present study.

*laura.simonelli@esrf.fr

¹M. Filippi, B. Kundys, S. Agrestini, W. Prellier, H. Oyanagi, and N. L. Saini, *J. Appl. Phys.* **106**, 104116 (2009).

²K. Ishizaka, T. Arima, Y. Murakami, R. Kajimoto, H. Yoshizawa, N. Nagaosa, and Y. Tokura, *Phys. Rev. Lett.* **92**, 196404 (2004).

³G. Blumberg, M. V. Klein, and S.-W. Cheong, *Phys. Rev. Lett.* **80**, 564 (1998).

⁴H. Woo, A. T. Boothroyd, K. Nakajima, T. G. Perring, C. D. Frost, P. G. Freeman, D. Prabhakaran, K. Yamada, and J. M. Tranquada, *Phys. Rev. B* **72**, 064437 (2005).

⁵J. H. Jung, D.-W. Kim, T. W. Noh, H. C. Kim, H.-C. Ri, S. J. Levett, M. R. Lees, D. McK. Paul, and G. Balakrishnan, *Phys. Rev. B* **64**, 165106 (2001).

⁶R. Klingeler, B. Büchner, S.-W. Cheong, and M. Hücker, *Phys. Rev. B* **72**, 104424 (2005).

⁷G. Wu and J. J. Neumeier, *Phys. Rev. B* **67**, 125116 (2003).

⁸T. Nomura and J. I. Igarashi, *Phys. Rev. B* **71**, 035110 (2005).

⁹J. van den Brink and M. van Veenendaal, *Europhys. Lett.* **73**, 121 (2006).

¹⁰E. Collart, A. Shukla, J.-P. Rueff, P. Leininger, H. Ishii, I. Jarrige, Y. Q. Cai, S.-W. Cheong, and G. Dhalenne, *Phys. Rev. Lett.* **96**, 157004 (2006).

¹¹K. Ishii, K. Tsutsui, Y. Endoh, T. Tohyama, S. Maekawa, M. Hoesch, K. Kuzushita, M. Tsubota, T. Inami, J. Mizuki, Y. Murakami, and K. Yamada, *Phys. Rev. Lett.* **94**, 207003 (2005).

¹²Y. J. Kim, J. P. Hill, C. A. Burns, S. Wakimoto, R. J. Birgeneau, D. Casa, T. Gog, and C. T. Venkataraman, *Phys. Rev. Lett.* **89**, 177003 (2002).

¹³M. Z. Hasan, E. D. Isaacs, Z.-X. Shen, L. L. Miller, K. Tsutsui, T. Tohyama, and S. Maekawa, *Science* **288**, 1811 (2000).

¹⁴Y.-J. Kim, J. P. Hill, G. D. Gu, F. C. Chou, S. Wakimoto, R. J. Birgeneau, S. Komiya, Y. Ando, N. Motoyama, K. M. Kojima, S. Uchida, D. Casa, and T. Gog, *Phys. Rev. B* **70**, 205128 (2004).

¹⁵S. Huotari, T. Pylkkänen, G. Vankó, R. Verbeni, P. Glatzel, and G. Monaco, *Phys. Rev. B* **78**, 041102(R) (2008).

¹⁶G. Ghiringhelli, N. B. Brookes, E. Annese, H. Berger, C. Dallera, M. Grioni, L. Perfetti, A. Tagliaferri, and L. Braicovich, *Phys. Rev. Lett.* **92**, 117406 (2004).

¹⁷T. Learmonth, C. McGuinness, P.-A. Glans, J. E. Downes, T. Schmitt, L.-C. Duda, J.-H. Guo, F. C. Chou, and K. E. Smith, *Europhys. Lett.* **79**, 47012 (2007).

¹⁸J. P. Hill, G. Blumberg, Y.-J. Kim, D. S. Ellis, S. Wakimoto, R. J. Birgeneau, S. Komiya, Y. Ando, B. Liang, R. L. Greene, D. Casa, and T. Gog, *Phys. Rev. Lett.* **100**, 097001 (2008).

¹⁹L. Braicovich, L. J. P. Ament, V. Bisogni, F. Forte, C. Aruta, G. Balestrino, N. B. Brookes, G. M. De Luca, P. G. Medaglia, F. Miletto Granozio, M. Radovic, M. Salluzzo, J. van den Brink, and G. Ghiringhelli, *Phys. Rev. Lett.* **102**, 167401 (2009).

²⁰S. Wakimoto, H. Kimura, K. Ishii, K. Ikeuchi, T. Adachi, M. Fujita, K. Kakurai, Y. Koike, J. Mizuki, Y. Noda, K. Yamada, A. H. Said, and Y. Shvyd'ko, *Phys. Rev. Lett.* **102**, 157001 (2009).

²¹L. Simonelli, S. Huotari, M. Filippi, N. L. Saini, and G. Monaco, *Phys. Rev. B* **81**, 195124 (2010).

²²A. Shukla, J.-P. Rueff, J. Badro, G. Vanko, A. Mattila, F. M. F. de Groot, and F. Sette, *Phys. Rev. B* **67**, 081101 (2003).

²³S. H. Han, M. B. Maple, Z. Fisk, W. Cheong, A. S. Cooper, O. Chmaissem, J. D. Sullivan, and M. Marezio, *Phys. Rev. B* **52**, 1347 (1995).

²⁴S. Arumugam, N. Môri, N. Takeshita, H. Takashima, T. Noda, H. Eisaki, and S. Uchida, *Phys. Rev. Lett.* **88**, 247001 (2002); T. Sasagawa, Suryadijaya, K. Shimatani, and H. Takagi, *Physica B* **359–361**, 436 (2005); N. Takeshita, T. Sasagawa, T. Sugioka, Y. Tokura, and H. Takagi, *J. Phys. Soc. Jpn.* **73**, 1123 (2004).

²⁵E. Kaneshita and A. R. Bishop, *J. Phys. Soc. Jpn.* **77**, 123709 (2008).

- ²⁶L. Simonelli, N. L. Saini, S. Huotari, V. Giordano, and G. Monaco, *J. Appl. Phys.* (to be published).
- ²⁷R. Verbeni, T. Pykkänen, S. Huotari, L. Simonelli, G. Vankó, K. Martel, C. Henriquet, and G. Monaco, *J. Synchrotron Radiat.* **16**, 469 (2009).
- ²⁸P. Glatzel and U. Bergmann, *Coord. Chem. Rev.* **249**, 65 (2005).
- ²⁹H. Eisaki, S. Uchida, T. Mizokawa, H. Namatame, A. Fujimori, J. van Elp, P. Kuiper, G. A. Sawatzky, S. Hosoya, and H. Katayama-Yoshida, *Phys. Rev. B* **45**, 12513 (1992); A. Fujimori, F. Minami, and S. Sugano, *ibid.* **29**, 5225 (1984).
- ³⁰A. Sahiner, M. Croft, S. Guha, I. Perez, Z. Zhang, M. Greenblatt, P. A. Metcalf, H. Jahns, and G. Liang, *Phys. Rev. B* **51**, 5879 (1995).